Astron. Astrophys. 245, 587–592 (1991)

ASTRONOMY AND ASTROPHYSICS

# Unified NLTE model atmospheres including spherical extension and stellar winds

## II. EUV-fluxes and the He II-Zanstra discrepancy in central stars of planetary nebulae

**R. Gabler** [1], **R. P. Kudritzki** [1,3], **and R. H. Méndez** [1,2,3]

[1] Institut für Astronomie und Astrophysik, Scheinerstrasse 1, D(West)-8000 München 80, Federal Republic of Germany
[2] Instituto de Astronomia y Fisica del Espacio, C.C. 67, 1428 Buenos Aires, Argentina
[3] Max-Planck-Institut für Astrophysik, Karl-Schwarzschildstrasse 1, D(West)-8046 Garching bei München, Federal Republic of Germany

Received November 7, accepted December 1, 1990

**Abstract.** A large grid of unified NLTE model atmospheres including radiation driven winds and spherical extension is computed for central stars of planetary nebulae (CSPN) in the effective temperature range from 40000 K to 100000 K. The calculated energy distributions are used to investigate the long-standing problem of the "Zanstra-discrepancy". It is shown that the increase of EUV flux in the unified models, caused by the presence of the wind velocity field in the layers of He II-groundstate continuum formation leads to much better agreement with the observations than was the case before, when plane-parallel hydrostatic models were used. However, for a significant fraction of the Central Stars investigated (45%) the computed flux is still about 1 dex too small. The remaining discrepancies are attributed to additional EUV-photons generated by shocks in the radiation driven winds. The ad hoc assumption of a blackbody energy distribution for $\lambda < 228$ Å using an effective temperature determined from the photospheric NLTE analysis of hydrogen and helium lines provides an excellent empirical description of the observed EUV flux.

**Key words:** model atmospheres – central stars of planetary nebulae – stellar winds.

### 1. Introduction

The oldest and still most frequently used method of estimating surface temperatures of central stars of planetary nebulae (CSPN) is that proposed by Zanstra (1931) and further developed by Harman & Seaton (1966). The fluxes in nebular emission lines such as H$\beta$ or He II 4686 are measured and then by means of recombination theory transformed into numbers of stellar photons ionizing H or $He^+$, respectively. Combined with the observed stellar visual flux a very temperature sensitive measure of the shape of the CSPN energy distribution is obtained (in principle the "far-UV-optical" colour) yielding the "H-Zanstra" and the "He II-Zanstra" temperatures, which are usually denoted by $T_Z$(H) and $T_Z$(He II).

Zanstra's (1931) paper already contains one example (NGC 7009) of what later came to be known the "Zanstra discrepancy", $T_Z$(He II) is in many cases much higher than $T_Z$(H). A recent review is given by Kaler (1989).

Most Zanstra temperatures in the literature have been calculated assuming blackbody stellar energy distributions. In consequence the Zanstra discrepancy can be attributed to one (or both) of the following reasons:

a) The nebula is optically thick in the He II-Lyman continuum, but is not absorbing all the H-Lyman continuum photons: $T_Z$(H) is a lower limit and $T_Z$(He II) is closer to the truth.

b) The stellar energy distribution shows a strong excess of $He^+$ ionizing photons over that indicated by blackbodies, therefore $T_Z$(He II) using blackbodies is too high. Adequate support for this explanation requires the production of realistic model atmosphere, capable of showing the proposed excess of $He^+$ ionizing photons. Given the high temperatures of CSPN, such models clearly have to be in non-LTE.

When the first non-LTE plane-parallel model atmospheres for CSPN became available, it turned out that they *increase* the Zanstra discrepancy (see e.g. the discussion by Heap 1977), because their energy distributions show a strong *absorption* edge at the He II-Lyman limit. These models give more or less the same $T_Z$(H) as blackbodies.

One way of clarifying the situation is to obtain direct information about surface temperatures from the stellar spectra. For this purpose, the basic stellar parameters ($T_{\rm eff}$, log $g$, photospheric He abundance) can be derived by fitting the stellar H and He absorption lines with theoretical profiles calculated from plane-parallel non-LTE models (Méndez et al. 1988a, 1988b, 1990; Mc Carthy et al. 1990). Although these models have several limitations (plane-parallel, hydrostatic and radiative equilibrium, H and He only), the derived $T_{\rm eff}$s are reliable, because they are based on spectral features formed deep in the photosphere where sphericity, hydrodynamics and metal-line blanketing effects are not expected to introduce large errors. By contrast, the $He^+$ ionizing continuum is formed at much higher layers, where the

*Send offprint requests to:* R.P. Kudritzki

limitations of the plane-parallel, hydrostatic models are a fundamental shortcoming.

A comparison of the spectroscopic $T_{\rm eff}$ s with Zanstra temperatures (Kaler 1989; Kudritzki & Méndez 1989) shows that normally the inequality

$$T_Z(\mathrm{H}) < T_{\rm eff} < T_Z(\mathrm{He\,II}) \qquad (1)$$

holds. This comparison includes the effect reported by Husfeld et al. (1984), where an emission edge at 228 Å was found for plane-parallel and hydrostatic models of hot CSPN ($T_{\rm eff} \geqq 80\,000$ K, see also Clegg & Middlemass 1987) close to the Eddington-limit. However, this particular NLTE-effect, although helpful does not fully solve the problem, because it occurs only in a very restricted region of the ($\log g$, $T_{\rm eff}$)-diagram, where small numbers of stars are to be found according to the photospheric analysis. The inequality (1) implies that *both* arguments (a) and (b) above are, to some extent, correct. In a separate paper (Méndez et al. 1991) we carefully discuss the available evidence about optical thickness and support the idea that many PN do not absorb all the H-Lyman continuum photons produced by their central stars. In the present paper we concentrate on the remaining discrepancy between $T_{\rm eff}$ and $T_Z$(He II), and investigate to what extent the improved "unified" NLTE model atmospheres including winds and sphericity developed recently by Gabler et al. (1989) can explain it.

The ultimate goal, of course, is to arrive at model atmospheres that simultaneously fit all spectral features (lines and continuum) either directly observed or inferred from the nebular spectrum. We expect to show that unified models are a useful step towards that goal.

## 2. Unified model atmospheres

For the calculation of theoretical CSPN emergent continuum fluxes, we have used the recently developed "unified" model atmospheres (Gabler et al. 1989). These non-LTE models are spherically extended, in radiative equilibrium and include the hydrodynamic density and velocity structure as given by the improved theory of radiation driven winds of Pauldrach et al. (1986). The entire sub- and supersonic atmosphere is treated in this way, without introducing an artificial division between "photosphere" and "wind".

In principle, the only input needed for these calculations is a set of values for the stellar effective temperature $T_{\rm eff}$, surface gravity $\log g$, stellar radius $R_*$ and photospheric He abundance. In the ideal case, a hydrodynamic code is run, using force multipliers $k, \alpha, \delta$ (cf. Pauldrach et al. 1986; Pauldrach 1987; Pauldrach et al. 1990; Kudritzki et al. 1989) determined self-consistently from the 4 basic stellar parameters just mentioned. The emergent continuum flux and line profiles then follow from detailed non-LTE multi-level calculations in the whole atmosphere, treating the contribution of subsonic and supersonic layers to the emergent flux and lines in the correct self-consistent, *unified* way.

Such detailed calculations were made for the bright O4f star $\zeta$-Puppis (Pauldrach 1987; Puls 1987; Gabler et al. 1989), with very encouraging results:

1. unified models produce much more continuum flux in the infrared $\lambda > 50\,000$ Å, in good agreement with the observations. And specially

2. shortward of 228 Å, the emergent flux in the unified model is substantially increased relative to the plane-parallel hydrostatic case. The reason is a strong depopulation of the He II ground state in the atmospheric region, where the continuum shortward of 228 Å becomes optically thin. This depopulation is a wind effect, caused by a velocity induced Doppler shift which produces a desaturation of the He II Lyman-$\alpha$ resonance line. More details are given in Gabler et al. (1989, appendix).

Gabler et al. also showed that the unified models are able, in principle to reproduce the observed stellar "wind" He II 4686 emissions, as well as the "photospheric" H$\gamma$ and He II 4541 absorptions in the spectra of Of-type CSPN.

These positive results prompted us to check if we could remove – or at least reproduce – the discrepancy between the spectroscopic $T_{\rm eff}$ and $T_Z$(He II) for CSPN using unified models. In order to avoid the enormous computational effort required to calculate a large grid of fully self-consistent unified models, we adopted the force multiplier parameters

$$k = 0.053,\ \alpha = 0.703,\ \delta = 0.052$$

(determined for $\zeta$-Puppis) for all models in our grid. This is certainly an approximation that will have to be improved in future work. At the moment, however, it is sufficient for a first investigation of the basic effects. Advantages and disadvantages of this procedure are discussed in Pauldrach et al. (1988). Table 1

**Table 1.** Grid of unified models and calculated Zanstra ratios

| $T_{\rm eff}$ | $\log g$ | $R/R_\odot$ | $M/M_\odot$ | $Z_{\rm He\,II}$ |
|---|---|---|---|---|
| 40 000 | 3.45 | 2.77 | 0.788 | 14.70 |
| | 3.5 | 2.55 | 0.750 | 21.78 |
| | 3.6 | 2.17 | 0.685 | 22.48 |
| | 3.7 | 1.87 | 0.637 | 22.51 |
| | 4.0 | 1.25 | 0.573 | 22.80 |
| | 4.4 | 0.765 | 0.536 | 22.47 |
| 50 000 | 3.85 | 1.74 | 0.78 | 23.24 |
| | 3.9 | 1.60 | 0.740 | 23.34 |
| | 4.0 | 1.365 | 0.680 | 23.45 |
| | 4.1 | 1.17 | 0.631 | 23.88 |
| | 4.2 | 1.02 | 0.602 | 23.94 |
| | 4.4 | 0.79 | 0.572 | 24.01 |
| | 4.8 | 0.482 | 0.536 | 23.85 |
| 70 000 | 4.45 | 0.863 | 0.766 | 25.60 |
| | 4.5 | 0.797 | 0.733 | 25.29 |
| | 4.6 | 0.681 | 0.673 | 24.26 |
| | 4.7 | 0.585 | 0.627 | 24.23 |
| | 5.0 | 0.397 | 0.575 | 24.27 |
| | 5.45 | 0.229 | 0.540 | 24.39 |
| 80 000 | 4.65 | 0.696 | 0.79 | 26.26 |
| | 4.7 | 0.643 | 0.757 | 26.17 |
| | 4.8 | 0.549 | 0.694 | 25.95 |
| | 5.0 | 0.409 | 0.610 | 25.17 |
| | 5.2 | 0.317 | 0.582 | 24.61 |
| | 5.5 | 0.220 | 0.558 | 24.52 |
| | 5.9 | 0.136 | 0.533 | 24.43 |
| 100 000 | 5.05 | 0.438 | 0.785 | 26.85 |
| | 5.1 | 0.405 | 0.755 | 26.81 |
| | 5.3 | 0.298 | 0.648 | 26.66 |
| | 5.7 | 0.178 | 0.577 | 26.28 |
| | 6.0 | 0.124 | 0.557 | 25.87 |
| | 6.2 | 0.097 | 0.546 | 25.60 |

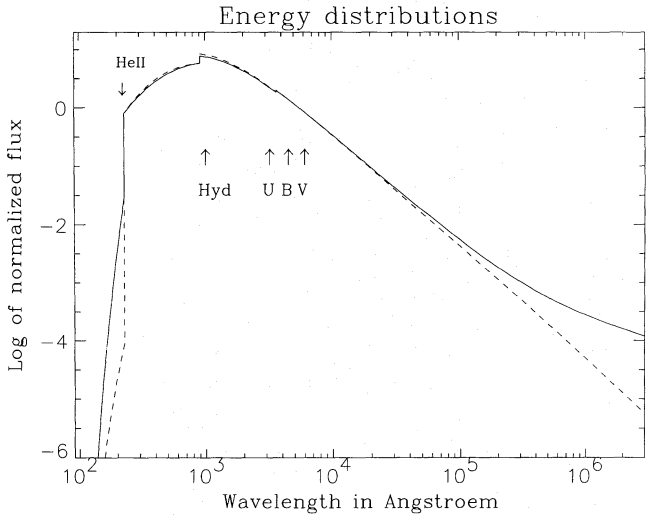


**Fig. 1a.** The energy distribution of an unified model (solid) with $T_{\rm eff} = 50\,000$ K, $\log g = 4.0$, $R_* = 1.365 * R_\odot$ and the plane-parallel, hydrostatic model (dashed) with the same $T_{\rm eff}$ and $\log g$. Note the difference in the EUV and IR spectral domain

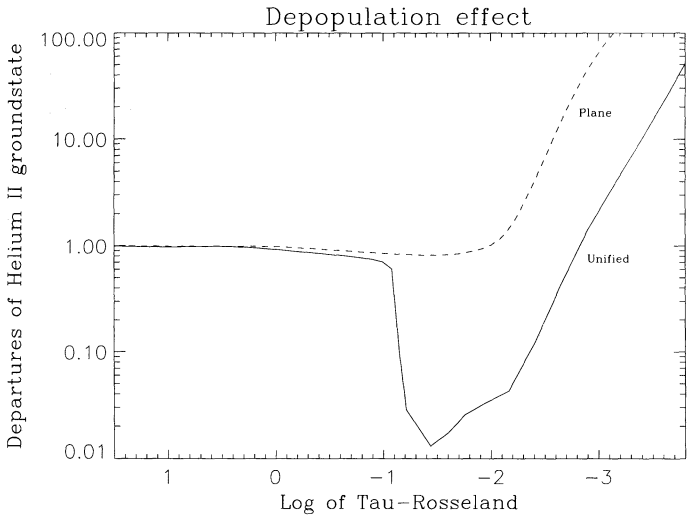


**Fig. 1b.** The He II-groundstate departure coefficient (for the same models as in Fig. 1a) as a function of Rosseland optical depth

lists the basic parameters of our grid models; in all cases a "normal" He abundance (0.09 by number fraction) was adopted.

In order to obtain suitable values of surface gravities and radii for each $T_{\rm eff}$, we extracted the luminosities and masses for each $T_{\rm eff}$ from the evolutionary tracks for post-AGB H-burners published by Schönberner (1989) and by Wood & Faulkner (1986). From $L$, $M$ and $T_{\rm eff}$ we obtained $\log g$ and $R_*$. We selected gravities going all the way from very low values, near the Eddington limit, to sufficiently high gravities covering the domain of observed CSPN as found by Méndez et al. (1988a) and Mc Carthy et al. (1990). Note that by using this procedure for combining gravities and radii we have assumed that all CSPN in our sample are burning H, which is not necessarily true. But the evolutionary tracks for He-burners of similar masses (Wood & Faulkner 1986) are not substantially different and for simplicity we have decided to neglect this possibility. Note also that in this paper, contrary to Gabler et al. (1989), we have adopted the stellar parameters $T_{\rm eff}$, $\log g$ and $R_*$ to be defined at Thomson optical depth unity. This simplifies the comparison with hydrostatic models and the results obtained from them.

Figure 1a shows the energy distribution for an unified model with $T_{\rm eff} = 50\,000$ K, $\log g = 4.0$ and $R_* = 1.365 * R_\odot$ compared with a hydrostatic model. This difference, which is caused by a depopulation of the He II groundstate as shown in Fig. 1b is obvious.

Figure 2 shows the location of our unified models in the ($\log g$, $T_{\rm eff}$) diagram. As we consider models closer to the Eddington limit, the winds become denser and mass-loss becomes more important. Figure 2 shows this effect: the full contour lines give the mass-loss rates, which become larger towards the Eddington-limit.

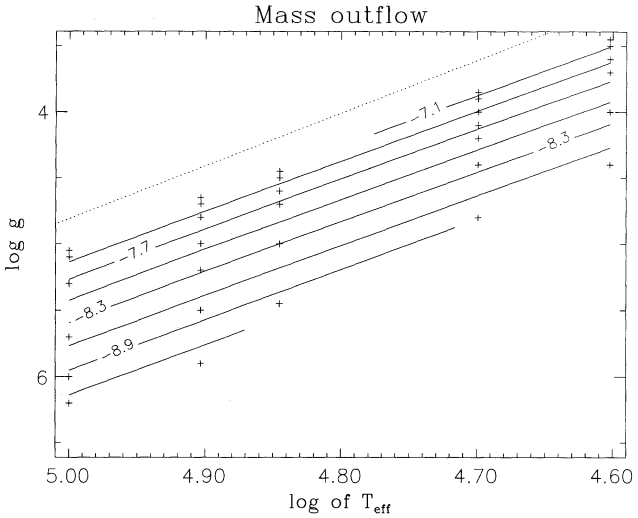


**Fig. 2.** The grid of unified models in the ($\log g$, $T_{\rm eff}$)-diagram. Each unified model is indicated with a plus sign. The full contour lines give the logarithms of mass-loss rate in solar masses per year. The dashed contour line shows the Eddington limit

## 3. A comparison between observed and computed He II-Zanstra ratios

From measurements of the nebular He II 4686 emission line flux and the stellar continuum flux at 5480 Å the "He II-Zanstra ratio" $H_{\rm He\,II}$ defined as

$$Z_{\rm He\,II} = \log \frac{\text{Number of He}^+ - \text{ionizing photons (cm}^{-2}\,\text{s}^{-1})}{\text{Stellar continuous flux at 5480 Å (erg cm}^{-2}\,\text{s}^{-1}\,\text{Hz}^{-1})} \quad (2)$$

can be determined as an observational quantity (see below). To compare with the predicted EUV model fluxes we have also computed $Z_{\rm He\,II}$ for each of the unified models (see Table 1). Moreover, to investigate the importance of winds and sphericity we have additionally computed a grid of "classical" plane-parallel, hydrostatic models and the corresponding Zanstra-ratios. (We have also calculated the analogous H-Zanstra ratios $Z_{\rm H}$ but since the differences between the unified and hydrostatic models are generally smaller than 0.05 dex we do not discuss these quantities further in this paper. We intend to publish a separate

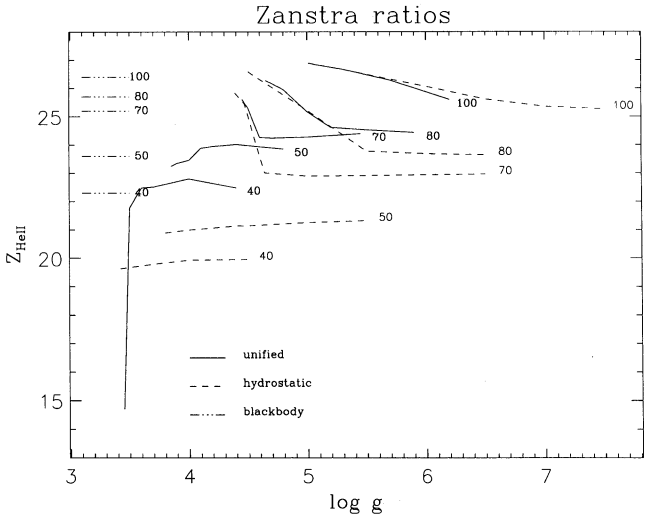


**Fig. 3a.** Zanstra ratios $Z_{\mathrm{He\,II}}$ for different effective temperature as a function of $\log g$ for unified (solid) and hydrostatic models (dashed). The corresponding blackbody curves are also shown (dashed-dotted)

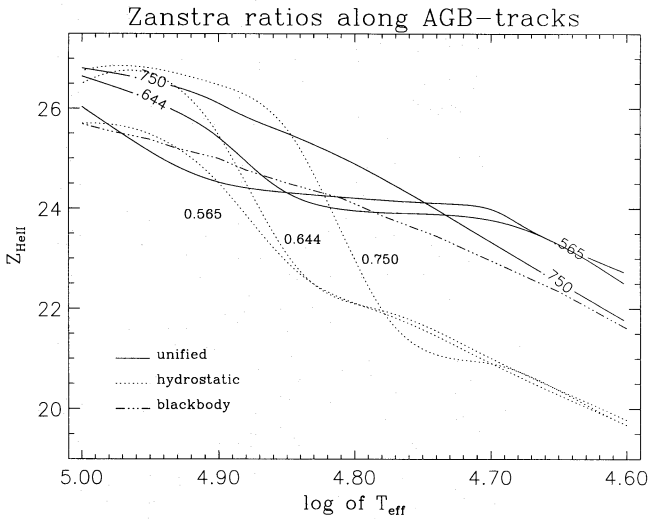


**Fig. 3b.** Zanstra ratios $Z_{\mathrm{He\,II}}$ predicted by unified (solid) and hydrostatic (dotted) models along the evolution of CSPN with constant mass (in solar units) towards higher temperatures. For comparison, the blackbody relation (dashed-dotted) is also shown

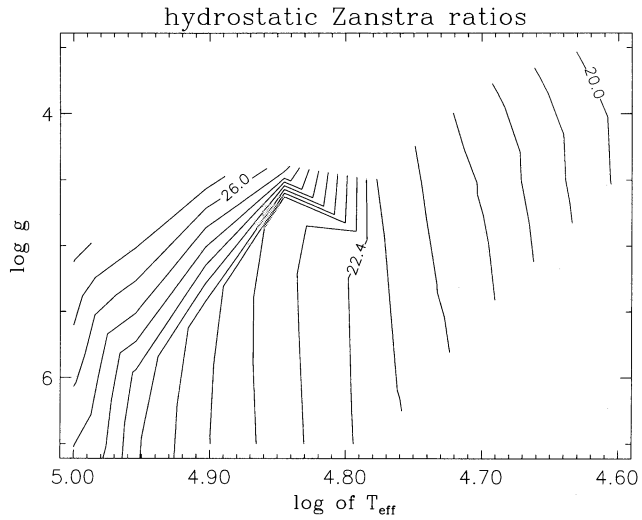


**Fig. 3c.** Iso-contour curves of $Z_{\mathrm{He\,II}}$ in the $\log g$, $T_{\mathrm{eff}}$-plane for plane-parallel, hydrostatic NLTE models. The increment between each iso-contour is 0.4 dex

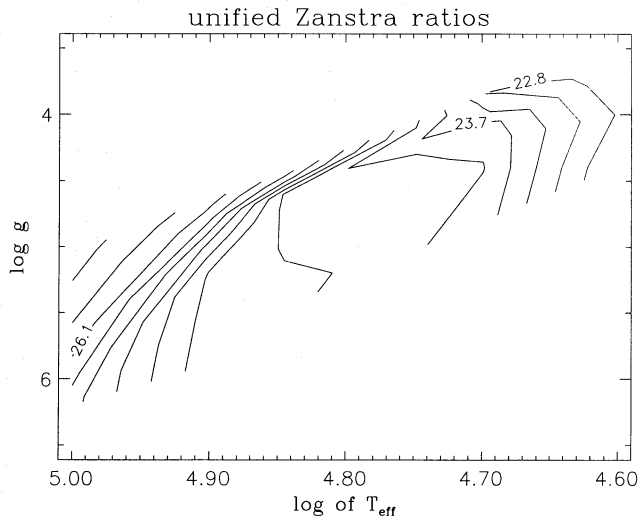


**Fig. 3d.** Iso-contour curves of $Z_{\mathrm{He\,II}}$ in the $\log g$, $T_{\mathrm{eff}}$-plane for unified NLTE models. The increment between each iso-contour is 0.3 dex

supplement paper giving full information about the calculated energy distributions).

The sequence in Fig. 3 gives an impression of the difference between the hydrostatic and unified models. Figure 3a shows that unified models can provide up to a factor of $10^3$ more He II-photons in the temperature range between 40 000 K and 70 000 K. The drop at 40 000 K for low gravity models close to the Eddington-limit is caused by the fact that here the radiation driven winds have a very low velocity and a very high density so that the He II-continuum is still optically thick far above those layers, where the depopulation of the ground state occurred. This means that close to the Eddington limit nearly similar "cool" CSPN can produce high and low $Z_{\mathrm{He\,II}}$. At 70 000 K the unified models with $\log g > 4.6$ yield still higher $Z_{\mathrm{He\,II}}$ than the hydrostatic models. The reason is that the winds at high gravities are very fast so that they can easily desaturate the He II resonance line and cause the depopulation effect, while – because of the high gravity – the He II-continuum is still formed above the sonic point. At low gravities and temperatures above or equal to 70 000 K, the He II-continuum is formed below the sonic point and the "emission-edge effect" found by Husfeld et al. (1984) in the hydrostatic models becomes important in the unified models as well. At 100 000 K the He II-continuum is purely photospheric for all gravities, which means that the differences between the hydrostatic and the unified case become negligible.

Figure 3b, which gives $Z_{\mathrm{He\,II}}$ along evolutionary tracks of constant mass, demonstrates the significant difference between the unified and the "classical" hydrostatic models in another way. Figures 3c and 3d showing iso-contours of $Z_{\mathrm{He\,II}}$ in the ($\log g$, $T_{\mathrm{eff}}$)-plane provide the tools for comparing observed and predicted $Z_{\mathrm{He\,II}}$ or for the determination of temperatures on the basis of both hydrostatic and unified models. They also reveal the well known fact that $Z_{\mathrm{He\,II}}$ can depend on both $T_{\mathrm{eff}}$ *and* $\log g$ (see Husfeld et al. 1984; Clegg & Middlemass 1987).

**Table 2.** Comparison between observed and calculated CSPN Zanstra ratios

| Star | $T_{\rm eff}$ ($10^3$) | log $g$ (cgs) | $Z^{\rm obs}$ | $Z^{\rm unif}$ | $Z^{\rm plane}$ | $Z^{\rm blackbody}$ |
|---|---|---|---|---|---|---|
| NGC 2392 | 47± 7 | 3.8±0.2 | 25.2±0.2 | $22.95^{+0.9}_{-0.8}$ | $20.6^{+0.8}_{-0.8}$ | $23.3^{+0.9}_{-1.1}$ |
| IC 3568 | 50± 5 | 4.0±0.2 | 23.6±0.2 | $23.55^{+0.3}_{-0.6}$ | $21.0^{+0.5}_{-0.5}$ | $23.6^{+0.5}_{-0.6}$ |
| IC 4637 | 50± 5 | 4.0±0.2 | 23.3±0.2 | $23.55^{+0.3}_{-0.6}$ | $21.0^{+0.5}_{-0.5}$ | $23.6^{+0.5}_{-0.6}$ |
| NGC 6210 | 50± 5 | 3.9±0.2 | 25.0±0.3 | $23.40^{+0.4}_{-0.7}$ | $21.0^{+0.5}_{-0.5}$ | $23.6^{+0.5}_{-0.6}$ |
| NGC 6891 | 50± 8 | 3.9±0.2 | 24.1±0.3 | $23.40^{+0.9}_{-1.0}$ | $21.0^{+0.8}_{-0.8}$ | $23.6^{+0.5}_{-0.6}$ |
| IC 2448 | 65± 5 | 4.8±0.2 | 25.8±0.2 | $24.20^{+0.1}_{-0.1}$ | $23.0^{+1.2}_{-0.8}$ | $24.9^{+0.6}_{-0.4}$ |
| NGC 1535 | 70± 5 | 4.6±0.2 | 25.2±0.2 | $24.30^{+1.9}_{-0.9}$ | $23.8^{+2.3}_{-0.4}$ | $25.2^{+0.3}_{-0.3}$ |
| NGC 3242 | 75± 5 | 4.7±0.2 | 25.9±0.2 | $25.20^{+1.2}_{-0.9}$ | $24.8^{+1.4}_{-1.9}$ | $25.5^{+0.2}_{-0.3}$ |
| NGC 1360 | 80± 5 | 5.4±0.2 | 25.9±0.2 | $24.55^{+0.8}_{-0.2}$ | $24.0^{+1.6}_{-0.7}$ | $25.7^{+0.2}_{-0.2}$ |
| NGC 4361 | 82± 5 | 5.5±0.2 | 26.4±0.2 | $24.65^{+0.9}_{-0.3}$ | $24.2^{+1.4}_{-0.7}$ | $25.8^{+0.2}_{-0.2}$ |
| NGC 7009 | 82±10 | 4.8±0.2 | 25.9±0.2 | $26.10^{+0.8}_{-1.6}$ | $24.2^{+1.8}_{-1.2}$ | $25.8^{+0.3}_{-0.5}$ |

In the next step, we compare both sets of calculations with observations. For this purpose, we have selected from the CSPN studied with the technique of photospheric analysis by Méndez et al. (1988a, 1990) and Mc Carthy et al. (1990) 11 objects surrounded by PN in which a nebular He II 4686 has been measured (see Table 2).

The "observed" $Z_{\rm He\,II}$ is obtained from

$$Z^{\rm obs}_{\rm He\,II} = 30.809 + \log F_{4686} + 0.4\,V + 0.17\,c + \log\left(\frac{\alpha_B({\rm He}^+)}{\alpha(4686)}\right) \quad (3)$$

where $F_{4686}$ is the observed nebular flux in He II 4686, in erg cm$^{-2}$ s$^{-1}$, $V$ is the apparent visual magnitude of the CSPN, $c$ is the logarithmic extinction at H$\beta$, and the $\alpha$s are recombination coefficients taken from Brocklehurst (1971) and Osterbrock (1974). The necessary data are given in Méndez et al. (1991) (see also Méndez, 1987). An additional comment is necessary concerning the gravities quoted in Table 2. Since Gabler et al. (1989) have shown that hydrostatic models produce slightly too strong Balmer absorption lines for models near the Eddington-limit, we have increased log $g$ for such cases by a small amount (typically $\Delta \log g = 0.1$ or smaller).

Using Figs. 3c, d and Table 2, observed and computed Zanstra ratios can be compared. The results are given in Table 2 and Fig. 4, where the uncertainties in the computed values are due to the uncertainties in $T_{\rm eff}$ and log $g$.

An inspection of Figs. 4a and 4b indicates that the use of the unified models generally improves the situation. In particular, for cooler objects such as IC 3568, IC 4637 and NGC 6891, where the hydrostatic models failed badly, the unified models come close to the observations. However, there remain objects like NGC 2392 and 6210, where the strong increase in the EUV flux produced in the unified models is still insufficient to reproduce the observed stellar fluxes inferred from the nebular He II 4686 recombination line. For the hotter objects the following situation is found. Half of the objects (NGC 1535, 3242, 7009) can be fitted by the unified models (at least within the error limits), but here the difference with the hydrostatic models is small and the latter are also marginally able to reproduce the observations due to the effect found by Husfeld et al. as discussed above. However, for the other half (IC 2448, NGC 1360, 4361) the models fail to produce sufficient EUV flux.

Figure 4c addresses the question, as to whether, from the observer's point of view a simple blackbody energy distribution in the EUV using the spectroscopic $T_{\rm eff}$ as stellar temperature is in agreement with the observed number of ionizing He II-photons. The result is striking. With a few exceptions (NGC 2392, 6210)

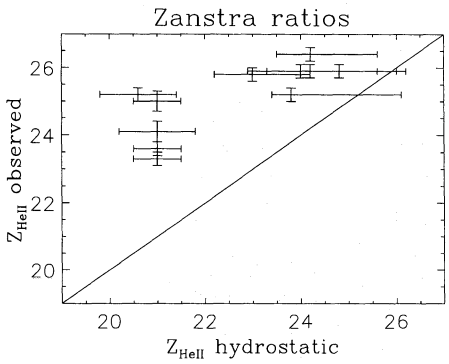


**Fig. 4a.** Observed $Z_{\rm He\,II}$ versus computed $Z_{\rm He\,II}$ using hydrostatic NLTE models

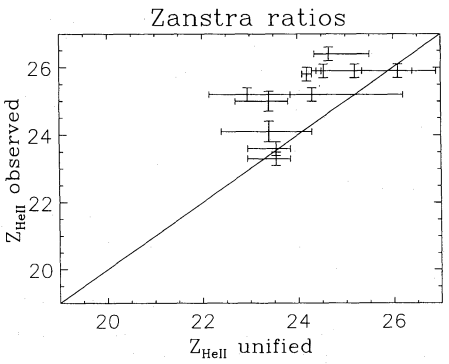


**Fig. 4b.** Observed $Z_{\rm He\,II}$ versus computed $Z_{\rm He\,II}$ using unified NLTE models

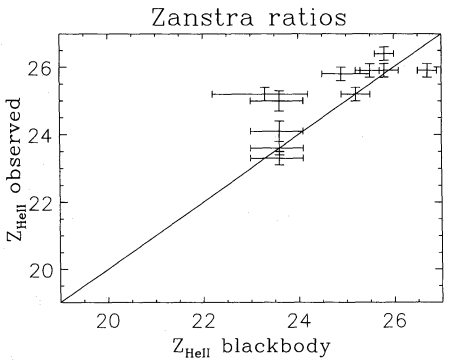


**Fig. 4c.** Observed $Z_{\rm He\,II}$ versus computed $Z_{\rm He\,II}$ using blackbodies

blackbodies appear to be a reasonable empirical description of the stellar EUV radiation field shortward of the He II-edge. Figure 3a indicates that even for $40\,000\,\mathrm{K} \leqq T_{\mathrm{eff}} \leqq 50\,000\,\mathrm{K}$ the simple blackbody law is a reasonable ad hoc approximation for the result of the complicated He II-depopulation effect caused by departures from LTE in expanding atmospheres. Thus it is not surprising that in the case of cool CSPN Fig. 4c and Table 2 lead to similar results for the sophisticated unified models and blackbodies. For the hotter CSPN the He II-opacity becomes weaker, the corresponding continuum more photospheric and the He II-depopulation effect less effective. This means that unified models give only small improvements and do not reach the level of full blackbody emission. In extremely discrepant cases (NGC 1360, 4361) they therefore also fail to provide sufficient EUV flux.

What might be the reason for the discrepancies that are left? First, we have to remember that these calculations were carried with ad hoc fixed force multiplier parameters $k, \alpha, \delta$ adjusted to self-consistent calculations for early massive O-stars. A self-consistent treatment of $k, \alpha, \delta$ at higher temperatures (which requires the inclusion of higher ionization stages in the line list of the radiation driven wind code) will certainly change the wind dynamics and thus the emergent He II-continuum. However, it would be surprising if this were to solve the factor of 10 discrepancies that we encounter in some cases. We, therefore, prefer an alternative hypothesis. From the study of massive O-stars we know that instabilities in their winds lead to shocks observable by X-ray emission. As recent test calculations have shown (Pauldrach et al. 1991 in prep.) these shocks can also provide a significant amount of EUV photons that would also contribute to the ionization of the nebulae. Of course, a very detailed analysis of the UV-spectra of CSPN with regard to their stellar wind properties (mass-loss rates, velocity field, shock amplitudes inferred from "turbulence") will be needed to investigate this hypothesis in the most discrepant cases. In addition, EUV-photons from stellar wind shocks might even be important for the non-discrepant cases. Here, it cannot be completely ruled out that the He II-groundstate depopulation effect is somewhat overestimated. Gabler et al. (1989) have shown that the effect depends on the radiation temperature of the incident continuous radiation at the frequency of the He II Lyman-$\alpha$ resonance line. It is important to note that our models neglect photospheric blocking by the numerous weak metal lines in the EUV and multi-line effects in the wind caused by velocity induced Doppler shifts (see Puls 1987), which might affect the radiation temperature of the pumping transition.

## 4. Conclusion

From the foregoing sections we conclude that unified NLTE model atmospheres lead to a substantial improvement in the description of the EUV radiation field of Central Stars of Planetary Nebulae when compared with the classical hydrostatic, plane-parallel NLTE models. In particular, in the temperature range between 40 000 K to 70 000 K the unified models lead to much better agreement when compared with observed stellar fluxes derived from the He II 4686 nebular recombination line. However, for a disturbingly large fraction of the Central Stars considered here ($\approx$45%) the improvements achieved with the unified atmospheres including winds and spherical extension are insufficient. In these cases the models still fail by one order of magnitude. We attribute this discrepancy to EUV photons produced in shocks generated by instabilities in the radiation driven winds, a mechanism that is not yet taken into account in our present models.

The ad hoc assumption of a blackbody energy distribution for $\lambda < 228$ Å with $T_{\mathrm{eff}}$ determined from the photospheric NLTE analysis of hydrogen and helium lines (Méndez et al. 1988, 1990; Mc Carthy et al. 1990) provides an excellent empirical description (with the exception of NGC 2392 and NGC 6210) of the observed stellar EUV flux. This conclusion, although an encouraging simplification for nebular analysis work, is somewhat painful from the viewpoint of the stellar atmosphere theorist. However, we take this as a challenge to develop a very complex theory further, until this very simple observational result is also reproduced.

*Acknowledgements.* R.H. Méndez wishes to thank the Max-Planck Institut für Astrophysik and the Universitätssternwarte München for hospitality and financial support. R. Gabler and R.P. Kudritzki gratefully acknowledge grants by the DFG (Ku 474/11 and 13) and by the BMFT (010R9008). The intense discussions with Dr. A.W.A. Pauldrach concerning the possible deficiencies of the unified models are also acknowledged.

## References

Brocklehurst M., 1971, MNRAS 153, 471
Clegg R.E.S., Middlemass D., 1987, MNRAS 228, 759
Gabler R., Gabler A., Kudritzki R.P., Puls J., Pauldrach A.W.A., 1989, A&A 226, 162
Harmann R.J., Seaton M.J., 1966, MNRAS 132, 15
Heap S.R., 1977, ApJ 215, 864
Husfeld D., Kudritzki R.P., Simon K.P., Clegg R.E.S., 1984, A&A 134, 139
Kaler J.B., 1989, Proc. IAU Symp. No. 131, Planetary nebulae, ed. S. Torres-Peimbert, Kluwer, Dordrecht, p. 229
Kudritzki R.P., Méndez R.H., 1989, Proc. IAU Symp. No. 131, Planetary nebulae, ed. S. Torres-Peimbert, Kluwer, Dordrecht, p. 273
Kudritzki R.P., Pauldrach A., Puls, J., Abbott D.C., 1989, A&A 219, 205
Mc Carthy J.K., Mould J.R., Méndez R.H., Kudritzki R.P., Husfeld D., Herrero A., Groth H.G., 1990, ApJ 351, 230
Méndez R.H., Kudritzki R.P., 1987, The 2nd Conference on Faint Blue Stars, IAU Coll. 95, eds. Davis Philip et al., L. Davis Press, Schenectady, New York, p. 191
Méndez R.H., Kudritzki R.P., Herrero A., Husfeld D., Groth H.G., 1988a, A&A 190, 113
Méndez R.H., Groth H.G., Husfeld D., Kudritzki R.P., Herrero A., 1988b, A&A 197, L25
Méndez R.H., Herrero A., Manchado A., 1990, A&A 229, 152
Méndez R.H., Kudritzki R.P., Herrero A., 1991, A&A (submitted)
Osterbrock D.E., 1974, Astrophysics of Gaseous Nebulae, Freeman, San Francisco, Table 2.8, p. 35
Pauldrach A., Puls J., Kudritzki R.P., 1986, A&A 164, 86
Pauldrach A.W.A., 1987, A&A 183, 295
Pauldrach A., Puls J., Kudritzki R.P., Méndez R.H., Heap S.R., 1988, A&A 207, 123
Pauldrach A., Kudritzki R.P., Puls J., Butler K., 1990, A&A 228, 125
Puls J., 1987, A&A 184, 227
Schönberner D., 1989, Proc. IAU Symp. No. 131, Planetary nebulae, ed. S. Torres-Peimbert, Kluwer, Dordrecht, p. 463
Wood P.R., Faulkner D.J., 1986, ApJ 307, 659
Zanstra H., 1931, Publ. Dom. Astrophys. Obs. 4, 209